

## **SYNTHESIS OF TITANIA NANOTUBES AND TITANIA NANOWIRES BY COMBINATION SONICATION-HYDROTHERMAL TREATMENT AND THEIR PHOTOCATALYTIC ACTIVITY FOR HYDROGEN PRODUCTION**

Indar Kustiningsih<sup>1,2</sup>, Slamet<sup>1</sup>, Widodo Wahyu Purwanto<sup>\*1</sup>

<sup>1</sup>*Chemical Engineering Department, Faculty of Engineering, Universitas Indonesia, Kampus Baru UI Depok 16424, Indonesia*

<sup>2</sup>*Chemical Engineering Department, Universitas Sultan Ageng Tirtayasa, Cilegon 42121, Indonesia*

(Received: July 2013 / Revised: June 2014 / Accepted: June 2014)

### **ABSTRACT**

Titania nanotubes (TiO<sub>2</sub> NT) and Titania nanowires (TiO<sub>2</sub> NW) were fabricated using TiO<sub>2</sub> Degussa P25 (TiO<sub>2</sub> P25) nanoparticle as precursors via a sonication-hydrothermal combination approach. The prepared catalysts were characterized by means of an X-ray diffraction (XRD), scanning electron microscope (SEM), transmission electron microscope (TEM), ultraviolet-visible diffuse reflectance spectroscopy (DRS) and the Brunauer-Emmett-Teller technique (BET). The photocatalytic activity of prepared catalysts was evaluated for photocatalytic H<sub>2</sub> evolution from an aqueous methanol solution. The results showed that activity of the catalyst not only depends on the morphology of its catalysts, but also on the crystallinity and surface area. Hydrogen production of TiO<sub>2</sub> NT was about three times higher than TiO<sub>2</sub> P25 and TiO<sub>2</sub> NW was two times higher than TiO<sub>2</sub>P25.

*Keywords:* Hydrogen production; Nanotubes; Nanowires; Photocatalytic; TiO<sub>2</sub>

### **1. INTRODUCTION**

Photocatalytic production of hydrogen from the dissociation of water represents a significant opportunity for the development of an alternative source of energy that is clean, abundant and storable. Since the first reported water splitting reaction over the TiO<sub>2</sub> photoelectrode (Fujishima & Honda, 1972), a variety of semiconductor materials have been developed for this purpose. Titanium oxide (TiO<sub>2</sub>) is well known as a material with excellent photocatalytic activity and has been investigated for hydrogen production. Compared to other photocatalysts for H<sub>2</sub> production, TiO<sub>2</sub> has received more attention because it is stable, corrosion-resistant, non-toxic, abundant and cheap (Fujishima & Honda, 1972; Hoffmann et al., 1995).

In recent years one-dimensional TiO<sub>2</sub> materials such as nanotubes and nanowires have attracted considerable attention due to their unique microstructure and promising functions (Morales & Liber, 1998). Many different methods and techniques have been developed to prepare 1-D TiO<sub>2</sub>-related materials, such as by the assisted-template method (Bavykin et al., 2006; Costa & Prado, 2009), by the sol-gel process (Kasuga et al., 1998), by electrochemical anodic oxidation (Gong et al., 2001, Sun et al., 2011, Zwillling et al., 1999), and by hydrothermal treatment (Chen & Mao, 2007; Dang et al., 2013; Kasuga et al., 1999; Wang et al., 2002; Wang et al., 2007; Zhang et al., 2003).

---

\* Corresponding author's email: widodo@che.ui.ac.id, Tel. +62-21786 3516, Fax. +62-21786 3515  
Permalink/DOI: <http://dx.doi.org/10.14716/ijtech.v5i2.400>

Among those mentioned above, the hydrothermal method for synthesis  $\text{TiO}_2\text{NT}$  has been reported to be the most powerful technique, due to simplicity of synthesis, cost effectiveness and an environmentally innocuous route (Morgado et al., 2007). Furthermore, the hydrothermal method can also be applied to prepare  $\text{TiO}_2$  NW (Jitputti et al., 2008; Ou & Lo, 2007; Asiah, et al., 2013). One of the disadvantages of the hydrothermal method is the long reaction duration needed, especially for  $\text{TiO}_2$  NW (Ou & Lo, 2007). Jitputti et al. (2008) reported that producing  $\text{TiO}_2$  NW by using hydrothermal method needed 75 hours. Therefore, the improvement of the hydrothermal synthesis process by shortening the reaction time is very important.

Many researchers have prepared  $\text{TiO}_2$  NT by the hydrothermal technique with the assistance of sonication (Wang et al., 2008; Viriya-Empikul et al., 2009; Zhu et al., 2001). Unfortunately, this improvement is complicated because the sonication treatment has been used *in situ* with the hydrothermal process (Wang et al., 2008). Furthermore, to the best of our knowledge, there are few reports on producing  $\text{TiO}_2\text{NW}$  by using a combination of the sonication and hydrothermal process and also the effect that morphologies of  $\text{TiO}_2$  nanostructures have on hydrogen production.

In this study a simple and fast method of combined sonication and hydrothermal treatment was proposed for the production of  $\text{TiO}_2\text{NT}$  and  $\text{TiO}_2\text{NW}$ . The physical properties of the  $\text{TiO}_2$  NT and  $\text{TiO}_2\text{NW}$  were studied in relation to their photocatalytic activity for  $\text{H}_2$  evolution.

## 2. EXPERIMENTAL

### 2.1. Catalyst preparation

$\text{TiO}_2$  Degussa P25 was used to synthesize  $\text{TiO}_2$  NT through the following procedures: 3 grams of  $\text{TiO}_2$  powders were dispersed in 150 mL of 10M NaOH and ultrasonicated for 15 minutes prior to hydrothermal treatment at  $130^\circ\text{C}$  for 12 hours using an autoclave, while for  $\text{TiO}_2$  NW was KOH (Potassium Hydroxide) and the temperature of hydrothermal treatment was  $150^\circ\text{C}$  for 15 hours. For comparison purposes, a second procedure was used to synthesize  $\text{TiO}_2$  NT and  $\text{TiO}_2$  NW. This was performed by the hydrothermal method without sonication. After the hydrothermal treatment, the precipitates were rinsed well with distilled water, then further rinsed with HCl (Hydrogen Chloride) and distilled water repeatedly until the pH value of the washing solution was lower than 7. The final products were obtained through centrifugation and further dried in a programmable furnace at  $150^\circ\text{C}$  then calcined or treated at a very high temperature of  $500^\circ\text{C}$ .

### 2.2. Catalyst characterization

The structure and morphology of products were characterized by several techniques. Powder X-ray diffraction (XRD) data were collected using a Philips PW 1710 diffractometer with  $\text{Cu K}\alpha$  radiation ( $\lambda = 1.5406\text{\AA}$  at a scan rate of  $0.025^\circ\text{s}^{-1}$ ) and the results were used to determine the phases present and their crystallite size. The crystallite size was calculated using a diffraction peak from Scherrer's formula (Weller, 1993). The transmission electron microscopy (TEM) analyses were conducted with a JEOL JEM-1400 electron microscope using a 120kV accelerating voltage. Morphological observations were performed on a JEOL JSM-6390A scanning electron microscope (SEM) equipped with an energy dispersive X-ray detector. Ultraviolet-visible diffuse reflectance spectroscopy (UV-vis DRS) was carried out using a Shimadzu 2450. The band gap energy of the samples was calculated using Kubelka-Munk equation (Yoong et al., 2009). The specific surface area of the samples was measured by BET of  $\text{N}_2$  adsorption in a Quantachrome Autosorb-6.

### 2.3. Photocatalytic activity test

The photocatalytic activity test was carried using a pyrex reactor equipped with six black light lamps (10W) as the photon source. The powder photocatalyst was suspended in a 10% methanol/water mixture at a concentration of  $1 \text{ gL}^{-1}$ . A magnetic stirrer was placed at the bottom of the reactor to ensure homogeneity of the suspension during reaction. The suspensions were then flushed with Argon (Ar) gas for 15 minutes to remove undesired gases such as oxygen and hydrogen. Hydrogen was analyzed by gas chromatography (GC) using a Shimadzu GC-8A equipped with a thermal conductivity detector, i.e. a stainless steel column packed with molecular sieves and an Ar carrier.

## 3. RESULTS AND DISCUSSION

Figure 1 shows SEM and TEM images of the prepared  $\text{TiO}_2\text{NT}$  and  $\text{TiO}_2\text{NW}$ . The sonication-hydrothermal treatment with NaOH (Sodium Hydroxide) as a solvent produced tube morphology (Figure 1(a)) and KOH (Potassium Hydroxide) as a solvent produced wire-like morphology (Figure 1(b)). TEM images show the difference between these catalysts,  $\text{TiO}_2\text{NT}$  has hollow morphology (Figure 1 (c)) and  $\text{TiO}_2\text{NW}$  has solid morphology (Figure 1 (d)).

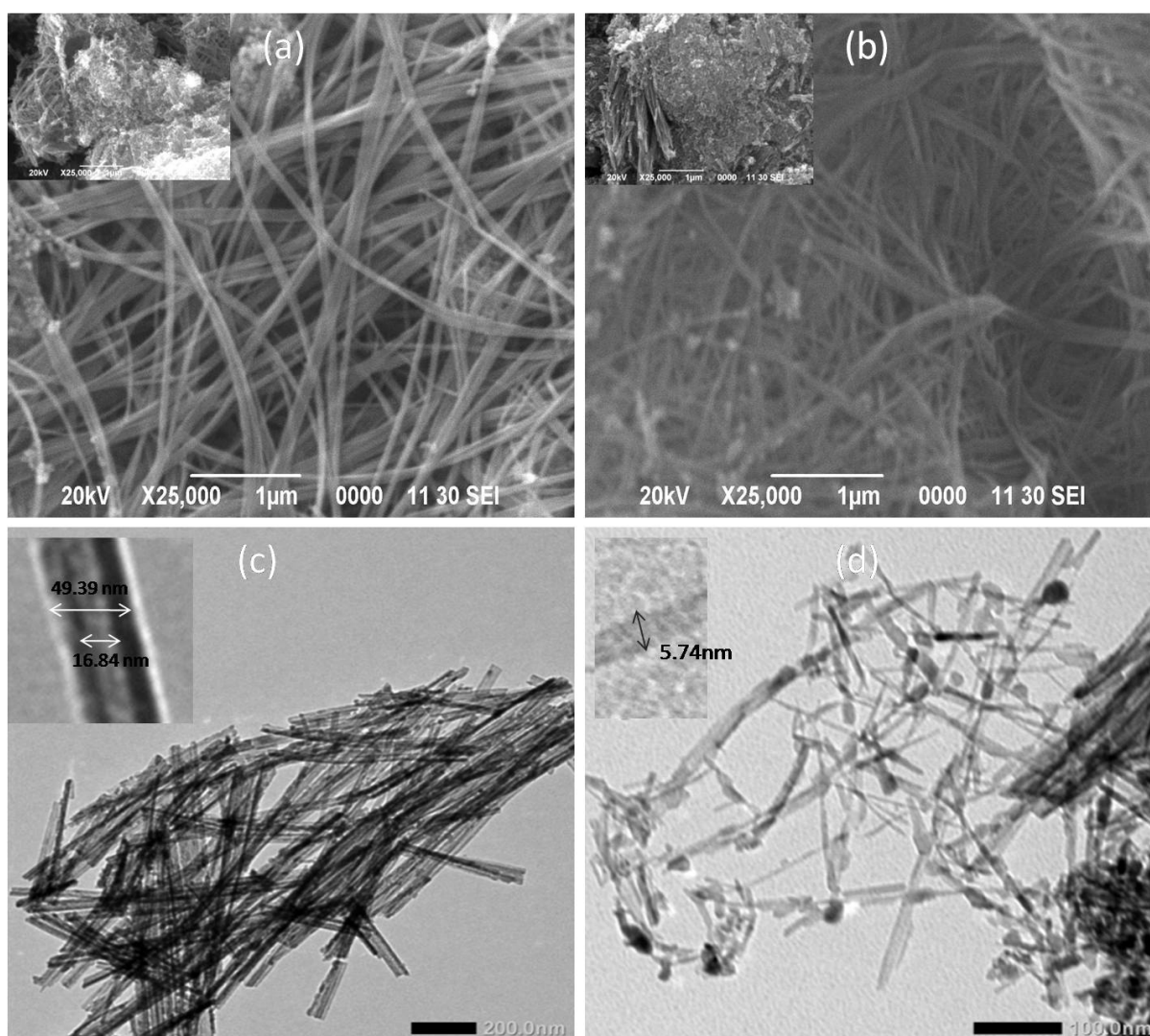


Figure 1 SEM images of: (a)  $\text{TiO}_2\text{NT}$ ; (b)  $\text{TiO}_2\text{NW}$ ; TEM images of: (c)  $\text{TiO}_2\text{NT}$ ; (d)  $\text{TiO}_2\text{NW}$ . Inset in (a) and (b) shows prepared samples after hydrothermal treatment without sonication treatment. Inset in (c) and (d) shows diameter of  $\text{TiO}_2\text{NT}$  and  $\text{TiO}_2\text{NW}$

The inner and outside diameter of TiO<sub>2</sub> NT was 16.84 nm and 49.39 nm respectively (the inset in Figure 1(c)), whereas the diameter of TiO<sub>2</sub> NW was 5.74 nm (the inset in Figure 1(d)). The difference in solvent that was used at hydrothermal treatment produced different morphology of catalysts. These results were confirmed by Yuan and Su who reported the difference morphology TiO<sub>2</sub> after hydrothermal process by using NaOH and KOH solvents (Yuan & Su, 2004). During the hydrothermal process, by using Ti-O-Ti, the bonds were broken to produce the sodium trititanates Na<sub>2</sub>Ti<sub>3</sub>O<sub>7</sub>. The sodium trititanate sheets were then peeled off into nanosheets and subsequently folded into nanotubes. By using KOH as a solvent, some of Ti-O-Ti bonds of Titania crystals are broken and layered as octatitanates (K<sub>2</sub>Ti<sub>8</sub>O<sub>17</sub>) that are formed on the titania surface along the (0 1 0) lattice plans of TiO<sub>2</sub>. Their (2 0 0) plans may parallel to the (0 1 0) lattice plan of TiO<sub>2</sub>. Further hydrothermal reactions cause the nanowires to grow out along the (0 1 0) direction (Yuan & Su, 2004).

The combination of sonication and hydrothermal processes can shorten the hydrothermal time to obtain nanotubes and nanowires. In this study by using this procedure could produce TiO<sub>2</sub> NT and TiO<sub>2</sub> NW in a short time. Without sonication treatment, the morphology of prepared samples after 12 hours of hydrothermal processes (NaOH as solvent) and 15 hours of hydrothermal (KOH as solvent) were not tube and wire shape, it can be seen as shown in the the inset in Figures 1(a) and 1(b). By using combination sonication hydrothermal treatment, nanotubes were obtained after 12-hour duration of hydrothermal processes, while otherwise nanowires were obtained after 15- hour duration. It is due to this sonication process that plays an important role in promoting intercalation or the insertion of the Na<sup>+</sup> (Sodium) or K<sup>+</sup> (Potassium) ions into lattices and breaking the Ti-O-Ti bonds without altering the morphology of TiO<sub>2</sub> Degussa P25. This result was much shorter than other researchers who obtained TiO<sub>2</sub> NT using the hydrothermal process without sonication. TiO<sub>2</sub> nanotubes usually obtained after 24-48 hours hydrothermal process at a temperature range of 110-150°C (Wang et al., 2008; Sreekantan & Wei, 2009). Other researchers reported TiO<sub>2</sub> NW was synthesized through a one-step hydrothermal process at 100-250°C for 24-72 hours (Yuan & Su, 2004). Viriya-empikul et al. (2009) synthesized TiO<sub>2</sub> NT and TiO<sub>2</sub> NW by using a combination of the sonication and hydrothermal process, but they still needed 3 days for the hydrothermal process at a temperature range between 90-180°C (Viriya-empikul et al., 2009).

Table 1 Summary of Crystallite size, BET surface and band gap energies of samples

Photocatalysts	BET Surface Area, m <sup>2</sup> /g	Crystallite Size, nm	Band Gap Energy
TiO <sub>2</sub> P25	54	18	3.28
TiO <sub>2</sub> NT	123	13	3.29
TiO <sub>2</sub> NW	115	9	3.29

The results of this study indicated the largest specific surface area was obtained in the form of TiO<sub>2</sub> nanotubes. These can be observed from BET characterization results of these catalysts in Table 1. The specific areas of TiO<sub>2</sub> NT, TiO<sub>2</sub> NW and TiO<sub>2</sub> P25 were 123 m<sup>2</sup>/g, 115 m<sup>2</sup>/g and 54 m<sup>2</sup>/g, respectively. The hollow shape on TiO<sub>2</sub> NT provided a high specific surface area that was greater than the wire shape on the TiO<sub>2</sub> NW and the nanoparticles on the TiO<sub>2</sub> P25. Although the TiO<sub>2</sub> NW did not have a hollow shape, its surface area was closer to that of the TiO<sub>2</sub> NT. This was due to the TiO<sub>2</sub> NW being formed in a porous condition. It can be shown in the TEM characterization, the tube wall of nanotubes (Figure 1(c)) were black, while the TiO<sub>2</sub> NW looked like a porous structure in diameter (Zhen, et al., 2013).

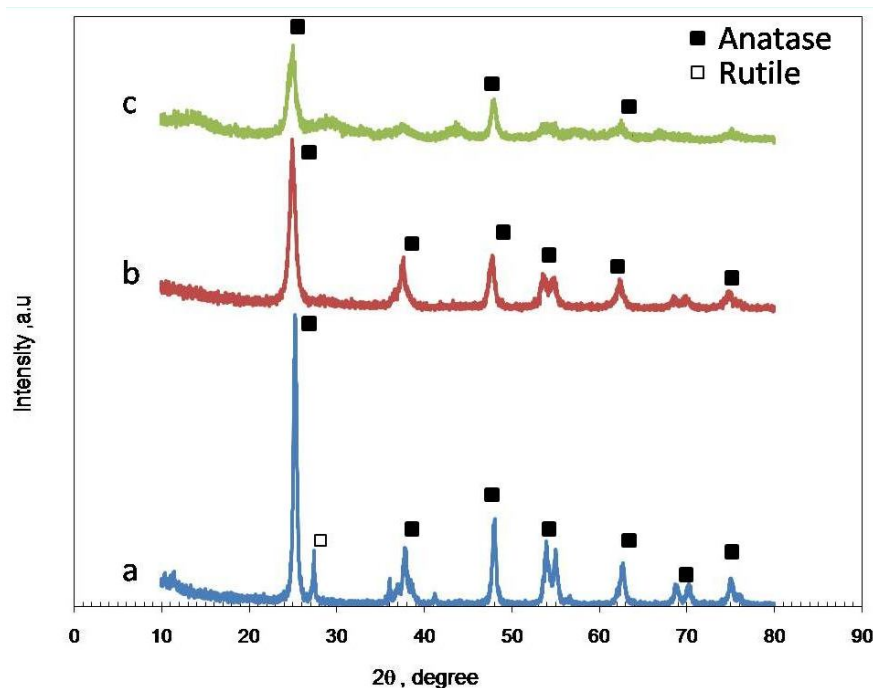


Figure 2 XRD patterns of: (a) TiO<sub>2</sub> P25; (b) TiO<sub>2</sub> NT; (c) TiO<sub>2</sub> NW

The phase composition, crystallite size and crystallinity of TiO<sub>2</sub> were reported to have a greater influence on the splitting of the water molecule. Therefore, XRD analyses of the samples were conducted. Figure 2 gives the XRD patterns of prepared sample (TiO<sub>2</sub> P25, TiO<sub>2</sub> NT and TiO<sub>2</sub> NW). The prepared catalysts annealed at temperatures in the region of 500°C in order to reveal the changes in phase structure and crystallite size caused by high temperature treatment. It was found that only the anatase phase was formed after calcination of the samples. A rutile peak at  $2\theta = 28.8$  was shown only by TiO<sub>2</sub> Degussa P25. It indicates that both of TiO<sub>2</sub> NT and TiO<sub>2</sub> NW exhibited the completely crystalline structure of anatase TiO<sub>2</sub> but TiO<sub>2</sub> P25 consisted of mixed anatase and rutile.

The XRD pattern of the calcined TiO<sub>2</sub> NW is shown at Figure 2(c). It was found that the intensity of diffraction lines corresponded to the TiO<sub>2</sub> anatase. The diffraction peaks of anatase phase are not sharp as the TiO<sub>2</sub> NT anatase peaks, indicating the crystallinity of the anatase phase of TiO<sub>2</sub> NT is higher than TiO<sub>2</sub> NW. This is due to the tubular shape on the TiO<sub>2</sub> NT that afforded receiving heat more evenly during the calcination process rather than the wire shape on the TiO<sub>2</sub> NW. The crystalline sizes of all samples are summarized in Table 1. Table 1 shows that the highest crystallite size was TiO<sub>2</sub> P25. The decrease in crystallite size after treatment was due to the hydrothermal process during which the TiO<sub>2</sub> P25 was transformed into an amorphous sodium trititanate. The formation of the anatase phase from the amorphous sodium trititanate occurred during the calcination treatments. Furthermore, the morphology of the prepared catalyst might affect the growth rate of the crystal.

The UV-visible diffuse reflectance spectra for samples calcined at 500°C are shown in Figure 3. For comparison purposes, the spectrum of TiO<sub>2</sub> P25 is also displayed. Band gap energy of the samples has been calculated using Kubelka-Munk equation (Yoong et al., 2009). Energy band gap is obtained by extrapolating the plot of the absorption coefficient at the y-axis versus energy at the x-axis.

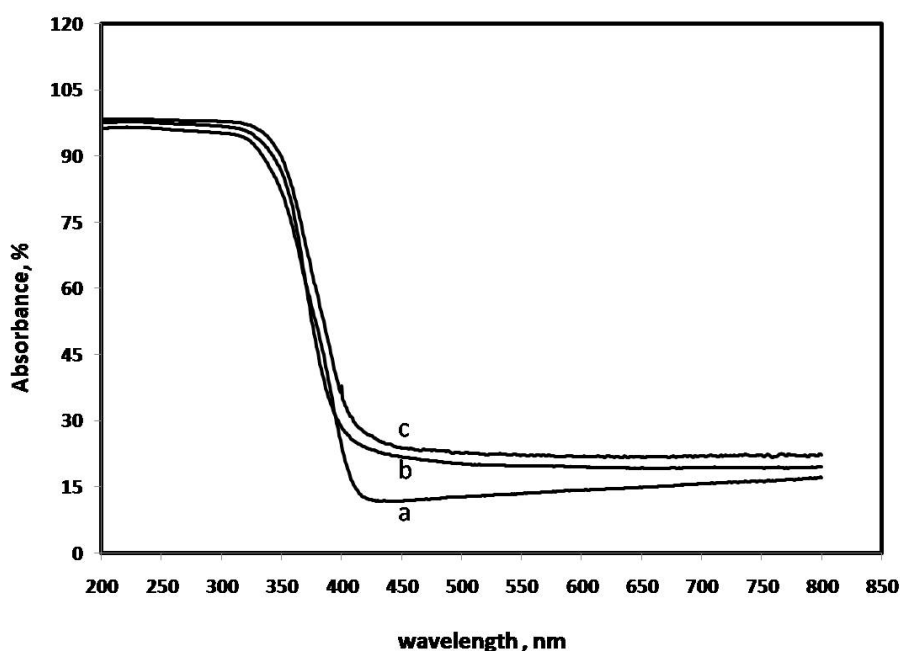


Figure 3 DRS characterization of: (a) TiO<sub>2</sub>P25; (b) TiO<sub>2</sub>NT; (c) TiO<sub>2</sub>NW

The results are shown in Table 1. There was no significant effect of morphology differences on the energy band gap. This was due to the crystal size of TiO<sub>2</sub> NT and TiO<sub>2</sub> that were quite similar to those shown in Table 1. Moreover, the EDX results in Table 2 indicated there were no impurities which could influence the energy band gap level.

Table 2 The EDX analysis for TiO<sub>2</sub> nanotubes and TiO<sub>2</sub> nanowires

Samples	%Ti	%O	%Na	%K
TiO <sub>2</sub> nanotubes	45.32	47.87	3.7	-
TiO <sub>2</sub> nanowires	48.67	46.54	-	4.79

Figure 4 illustrates the comparison of photocatalytic activity between TiO<sub>2</sub> in the form of nanotubes, nanowires and nanoparticles. It was found that TiO<sub>2</sub> nanotubes exhibited the highest activity rates in comparison with other samples. The hydrogen production of TiO<sub>2</sub> NT was almost three times higher than the TiO<sub>2</sub> P25 nanoparticles and the TiO<sub>2</sub> NW were two times higher than the TiO<sub>2</sub> P25. Even though the crystallinity factors of TiO<sub>2</sub> NT and TiO<sub>2</sub> NW were lower than the TiO<sub>2</sub> P25, their respective activities were higher than TiO<sub>2</sub> P25. This was due to the specific surface area that also influenced the calibrated activity of the samples. The large specific area could accommodate more reactions and also could be attributed to reducing recombination (Su *et al.*, 2006).

The difference of the specific surface area between TiO<sub>2</sub> NT and TiO<sub>2</sub> NW were not overly significant, but their activity in terms of hydrogen production was different. This is probably attributed to the tube shape on the TiO<sub>2</sub> NT that allows for more effective contact between active site, photons and water molecules, which then results in better photocatalytic activity. Sun *et al* (2006) reported that the tubular structure facilitated faster electron transfer due to reduced grain boundaries, which was expected to improve charge separation in photocatalytic reactions. This result indicated that morphology of TiO<sub>2</sub> plays an important role in generating hydrogen from water splitting.

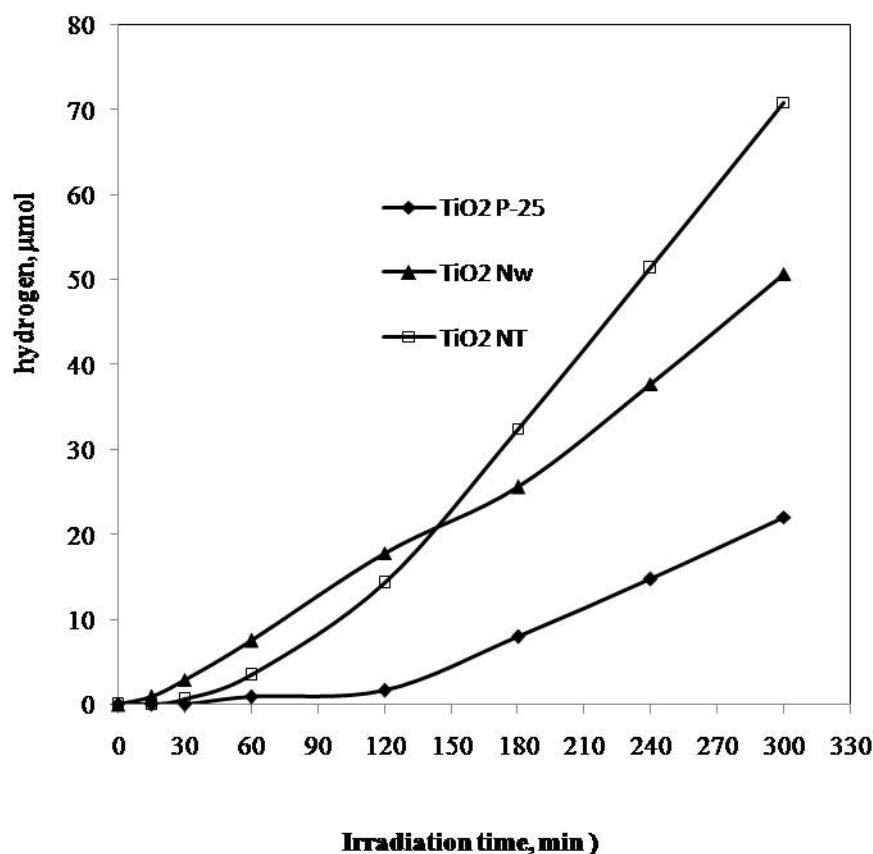


Figure 4 Hydrogen evolution over TiO<sub>2</sub> NT, TiO<sub>2</sub> NW and TiO<sub>2</sub> P25 nanoparticles (V<sub>solution</sub> = 500 ml, catalyst = 0.5 g, light source UV, Methanol concentration = 10% v)

This result was primarily attributed to the unique one-dimensional nanotubular structure. This one-dimensional tubular structure facilitated faster transfer of electrons due to reduced grain boundaries and this occurrence was expected to improve charge separation in photocatalytic reactions.

#### 4. CONCLUSION

TiO<sub>2</sub> Nanotubes and TiO<sub>2</sub> Nanowires with high crystallinity and large surface area were successfully produced by a simple combined sonication and hydrothermal method. A shorter duration of TiO<sub>2</sub> nanotubes and TiO<sub>2</sub> nanowires formations was achieved through this method with a 12-hour duration for TiO<sub>2</sub> NT and 15-hour duration for TiO<sub>2</sub> NW. The morphology of catalysts played a significant role in the specific surface area and their crystallinity. It also possibly affected the photon and charge transfer. Photocatalytic hydrogen production using TiO<sub>2</sub> nanotubes achieved a better performance level than TiO<sub>2</sub> nanowires.

#### 5. ACKNOWLEDGEMENT

The main financial support from the Directorate General of Higher Education, Ministry of National Education Indonesia by HIBAH PASCA (1721/H2.R12.3/PPM.00 Penelitian /2010) is gratefully acknowledged.

## 6. REFERENCES

- Asiah, M.N., Mamat, M.H., Khusaimi, Z., Achoi, M.F., Abdullah, S., Rusop, M., 2013. Thermal Stability and Phase Transformation of TiO<sub>2</sub> Nanowires at Various Temperatures. *Microelectronics Engineering*, Volume 108, pp. 134–137
- Bavykin, D.V., Friedrich, J.M., Walsh, F.C., 2006. Protonated Titanates and TiO<sub>2</sub> Nanostructured Materials: Synthesis, Properties and Application. *Adv. Mater.* Volume 18, pp. 2807–2824
- Chen, X.B. Mao, S.S., 2007. Titanium Dioxide Nanomaterials: Synthesis, Properties, Modification and Applications. *Chem. Rev.* Volume 107, pp. 2891–2959
- Costa, L.L., Prado, A.G.S., 2009. TiO<sub>2</sub> Nanotubes as Recyclable Catalyst for Efficient Photocatalytic Degradation of Indigo Carmine Dye. *J. Photochem. Photobiol. A.* Volume 201, pp. 45–49
- Dang, H. Dong, X., Zhang, Y., Hampshire, S., 2013. TiO<sub>2</sub> Nanotubes Coupled with Nano-Cu(OH)<sub>2</sub> for Highly Efficient Photocatalytic Hydrogen Production. *Int. J. Hydrogen Energy.* Volume 38, pp. 2126–2135
- Fujishima, K. Honda., 1972. Electrochemical Photolysis of Water at a Semiconductor Electrode. *Nature* Volume 238. pp. 37–38
- Gong, D., Grimes, C.A., Varghese, O.K., Hu, W., Singh, R.S., Chen, Z., Dickey, E.C., 2001. Titanium Oxide Nanotube Arrays Prepared by Anodic Oxidation. *J. Mater. Res.* Volume 16, pp. 3331–3334
- Hoffmann, M.R., Martin, S.T., Choi, W., Bahnemann, D.W., 1995. Environmental Application of Semiconductor Photocatalysis. *Chem. Rev.* Volume 95, pp. 69–96
- Jin, Z., Meng, F., Jia, Y., Luo., T., Liu, J., Sun, B., Wang, J., Liu, J., Huang, X., 2013. Porous TiO<sub>2</sub> Nanowires Derived from Nanotubes: Synthesis Characterization and their Enhanced Photocatalytic Properties. *Microporous and Mesoporous Materials.* Volume 181, pp. 146–153
- Jitputti, J., Suzuki, Y., Yoshikawa, S., 2008. Synthesis of TiO<sub>2</sub> Nanowires and their Photocatalytic Activity for Hydrogen Evolution. *Catal. Commun.* Volume 9, pp. 1265–1271
- Kasuga, T., Hiramatsu., M., Hoson., A., Sekino, T., Nihara, K., 1999. Titania Nanotubes Prepared by Chemical Processing. *Adv. Mater.* Volume 11, pp. 1307–1311
- Kasuga, T., Hiramatsu., M., Hoson., A., Sekino, T., Nihara, K., 1998. Formation of Titanium Oxide Nanotubes. *Langmuir.* Volume 14, pp. 3160–3163
- Morales, A.M., Liber, C.M., 1998. A Laser Ablation Method for the Synthesis of Crystalline Semiconductor Nanowires. *Science.* Volume 279, pp. 208–211
- Morgado, E., de Abreu., M.A.S., Moure., G.T., Marinkovic., B.A., Jardim., P.M., Araujo, A.S., 2007. *Chem. Mater.* Volume 19, pp. 665–676
- Ou, H.H., Lo, S.L., 2007. Review of Titania Nanotubes Synthesized via the Hydrothermal Treatment: Fabrication, Modification and Application. *Sep. Purif. Technol.* Volume 58, pp. 179–191
- Sreekantan, S., Wei, L.C., 2009. Study on the Formation and Photocatalytic Activity of Titanate Nanotubes Synthesized via Hydrothermal Method. *J Alloy Compd.* Volume 1-2, pp. 436–442
- Sun, W., Zhang, S., Liu, Z., Wang, C., Mao, Z., 2006. Studies on the Enhanced Photocatalytic Hydrogen Evolution Over Pt/PEG–Modified TiO<sub>2</sub> Photocatalysts. *Int J. Hydrogen Energy.* Volume 31, pp 786–796



- Sun, Y., Wang, G., Yan, K., 2011. TiO<sub>2</sub> Nanotubes for Hydrogen Generation by Photocatalytic Water Splitting in a Two-compartment Photoelectrochemical Cell. *Int. J. Hydrogen Energy*. Volume 36, pp. 15502-15508
- Viriya-empikul, N., Charinpanitkul, T., Sano, N., Soottitantawat, A., Kikuchi, T., Faungnawakij, K., Tanthapanichakoon, W., 2009. Effect of Reaction and Sonication Pretreatment in the Hydrothermal Process on the Morphology of Titanate Nanostructure. *J Chem Eng Jpn*. Volume 42, pp. 234–237
- Wang, D., Zhou, F., Liu, Y., Liu, W., 2008. Synthesis and Characterization of Anatase TiO<sub>2</sub> Nanotubes with Uniform Diameter from Titanium Powder. *Mater. Lett*. Volume 62, pp. 1819–1822
- Wang, F.M., Shi, Z.S., Gong, F., Jiu J.T., Adachi, M., 2007. Morphology Control of Anatase TiO<sub>2</sub> by Surfactant-assisted Hydrothermal Method. *Chin. J. Chem. Eng*. Volume 15, pp. 754–759
- Wang, Y.Q., Hu, G.Q., Duan, X.F., Sun, H.L., Xue, Q.K., 2002. Microstructure and Formation Mechanism of Titanium Oxide Nanotubes. *Chem. Phys. Lett*. Volume 365, pp. 427–431
- Weller, H., 1993. Colloidal Semiconductor Q-particles Chemistry in the Transition Region between Solid State and Molecules *Angew. Chem. Int. Ed. Engl*. Volume 32, pp. 41–53
- Yoong, L.S., Chong, F.K., Duta, B.K., 2009. Development of Copper-doped TiO<sub>2</sub> Photocatalyst for Hydrogen Production under Visible Light. *Energy*. Volume 34, pp. 1652–1661
- Yuan, Z.Y., Su, B. L., 2004. Titanium Oxide Nanotubes, Nanofibers and Nanowires. *Colloid Surface A*. Volume 241, pp. 173–183
- Zhang, S., Peng, L.M., Chen, Q., Du, G.H., Dawson, G., Zhou, W.Z., 2003. Formation Mechanism of H<sub>2</sub>Ti<sub>3</sub>O<sub>7</sub> Nanotubes. *Phys. Rev. Lett*. Volume 91, pp. 256103
- Zhu, Y.C., Li, H.L., Koltypin, Y., Hacohebn, Y.R., 2001. Gedanken Sonochemical Synthesis of Titania Whiskers and Nanotubes. *Chem. Commun*. Volume 24, pp. 2616–2617
- Zwilling, V., Aucouturier, M., Darque-Ceretti, E., 1999. Anodic Oxidation of Titanium and TA6V Alloy in Chromic Media, an Electrochemical Approach. *Electrochim. Acta*. Volume 45, pp. 921–929